

# Ambient induced degradation and chemically activated recovery in copper phthalocyanine thin film transistors

Jeongwon Park,<sup>1</sup> James E. Royer,<sup>2</sup> Corneliu N. Colesniuc,<sup>3</sup> Forest I. Bohrer,<sup>2</sup> Amos Sharoni,<sup>3</sup> Sungho Jin,<sup>1</sup> Ivan K. Schuller,<sup>3</sup> William C. Trogler,<sup>2</sup> and Andrew C. Kummel<sup>2,a)</sup>

<sup>1</sup>Materials Science and Engineering Program, University of California, San Diego, 9500 Gilman Drive, La Jolla, California 92093, USA

<sup>2</sup>Department of Chemistry and Biochemistry, University of California, San Diego, 9500 Gilman Drive, La Jolla, California 92093, USA

<sup>3</sup>Department of Physics, University of California, San Diego, 9500 Gilman Drive, La Jolla, California 92093, USA

(Received 20 November 2008; accepted 7 June 2009; published online 12 August 2009)

The electrical degradation (aging) of copper phthalocyanine (CuPc) organic thin film transistors (OTFTs) was investigated. Thick (1000 ML) and ultrathin (4 ML) channel thicknesses were used in bottom contact OTFTs to correlate the electrical effects of aging with film microstructure. Proper TFT saturation behavior was unattainable in thick devices subject to ambient aging; however ultrathin devices were significantly less susceptible and maintained good saturation and subthreshold behavior. Therefore 1000 monolayer (ML) CuPc OTFTs were characterized in ambient air, clean dry air, clean humidified air, and NO<sub>x</sub> environments to isolate the ambient components that induce aging. Thick channel devices which had been aged in ambient air to the point of losing all saturation behavior could be restored to proper saturation behavior by exposure to clean humidified air. The data are consistent with aging resulting primarily from adsorption of strong oxidants from ambient air within the grain boundaries of the CuPc films. © 2009 American Institute of Physics. [DOI: 10.1063/1.3159885]

## I. INTRODUCTION

The recent demand for low cost, versatile electronic devices has stimulated interest in organic thin film transistors (OTFTs).<sup>1,2</sup> Application of OTFTs as chemical sensors has shown promise in the development of electronic noses and nerve agent detection.<sup>3–5</sup> A key issue regarding the widespread production of OTFTs is the long term stability and device integrity in ambient operating conditions.<sup>6–8</sup> Among the small molecule based OTFTs, pentacene OTFTs have received significant attention regarding instability to ambient components such as oxygen and humidity.<sup>9–13</sup> Several mechanisms have been proposed to explain this instability in pentacene OTFTs, including water adsorption in grain boundaries,<sup>11,12</sup> and oxygen generated impurities.<sup>14</sup> In these studies, the surface morphology of the pentacene films dramatically influenced the effects of the atmospheric contaminants. Similar correlations between surface morphology and sensor response has also been reported for thiophene based OTFTs.<sup>15</sup> Metal phthalocyanines (MPcs) are another well studied group of organic semiconductors, which have been applied for novel OTFT based sensors.<sup>16</sup> However, a limited number of studies have been reported concerning the degradation of OTFT performance where MPcs are employed as the organic active layer.<sup>6,17,18</sup> A systematic approach to isolating the cause of device degradation (“aging”) in copper phthalocyanine (CuPc) OTFTs can provide insight to the interactions of MPc films with atmospheric agents.

In this report, the effects of ambient induced aging are investigated for CuPc OTFTs with channel thicknesses ranging from 4 to 1000 monolayers (MLs). Adsorption and diffusion processes involving strong ambient oxidants (e.g., NO<sub>x</sub>) within the grain boundaries of the CuPc film is the most likely mechanism resulting in CuPc OTFT degradation. A process to counteract the electrical effects of aging via displacement of the strong oxidants is also investigated.

## II. EXPERIMENTAL DETAILS

### A. Electrode fabrication

Metal electrodes consisting of Ti (5 nm) and Au (45 nm) were patterned on heavily doped (100) *n*<sup>+</sup> Si wafers (common gate) with thermally grown 100 nm SiO<sub>2</sub> (gate oxide) from Nova Electronic Materials, Ltd. using photolithography and a bilayer photoresist lift-off process.<sup>19</sup> In the bilayer photoresist lift-off process, two different types of photoresist material with distinct etching rates were utilized: a polymethylglutarimide (PMGI) mixture with equal volumes of pure PMGI SF13 and PMGI SF3 solutions to create about 300 nm high undercut layer for the bottom resist layer and Microposit® S1818 photoresist for the 2 μm high top resist layer. The underlying PMGI resist layer develops nearly isotropically and etches faster in the Microposit® MF319 developer solution (Shipley Corp.) than the top layer S1818. Therefore, the amount of undercut is controlled precisely by the etching rate of PMGI. The electrodes consist of 45 pairs of interdigitated gold fingers forming a 5 μm channel length and 2 mm

<sup>a)</sup>Electronic mail: akummel@ucsd.edu.

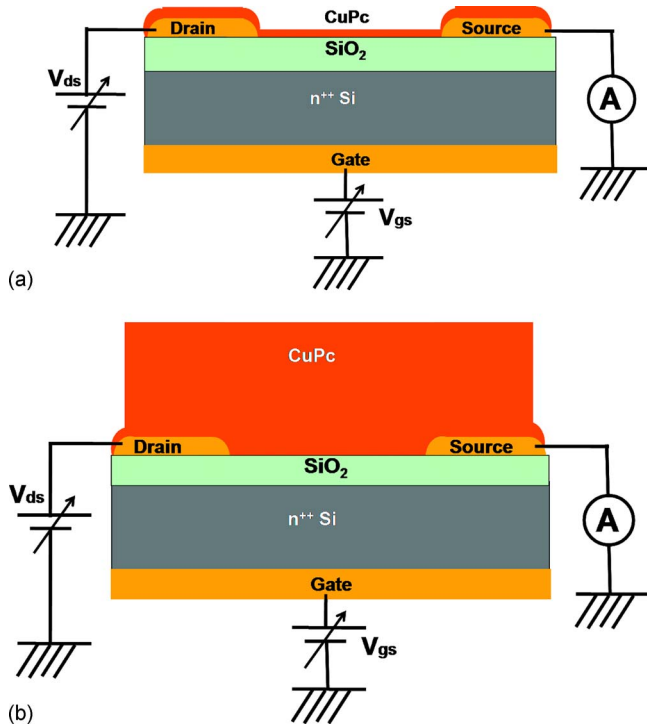


FIG. 1. (Color online) Schematic cross section of device structures (a) with a thin CuPc layer and (b) with a thick CuPc layer. The electrodes consist of 45 interdigitated fingers, with a 5  $\mu\text{m}$  channel length ( $L$ ) and channel width ( $W$ ) of 2000  $\mu\text{m}$ ;  $W/L=17,600$ .

channel width. Six pairs of electrodes were patterned on each substrate to verify reproducibility and increase yield.

## B. Thin film deposition

CuPc was purchased from Sigma-Aldrich and purified via multiple zone sublimations at 400  $^{\circ}\text{C}$  and  $10^{-5}$  torr for over 50 h with a yield over 70%. CuPc films with 4 ML to 1000 ML thickness were deposited on chips with six OTFT devices per chip to assess reproducibility. The CuPc was deposited by organic molecular beam deposition in a UHV chamber with a base pressure of  $1 \times 10^{-10}$  torr. The deposition rate of the CuPc films ranged from 0.3 to 0.5  $\text{\AA}/\text{s}$ , and the deposition pressure was  $1 \times 10^{-8}$  torr. Substrate temperature during deposition was held constant at 25  $^{\circ}\text{C}$ .

## C. Film characterization

Surface morphology was measured by atomic force microscopy (AFM) using a Nanoscope IV scanning microscope in tapping mode and a VEECO 200 kHz probe. The film thicknesses were measured during deposition with a quartz crystal microbalance, which was calibrated by AFM and low angle x-ray diffraction (XRD) measurements using a Rigaku RU-200B diffractometer with Cu  $K\alpha$  radiation. XRD revealed the films to be textured  $\alpha$  phase. The  $d$  spacing was 13.3  $\text{\AA}$  in accordance with previous measurements that show that the phthalocyanine molecules are oriented perpendicular to the substrate surface.<sup>20</sup>

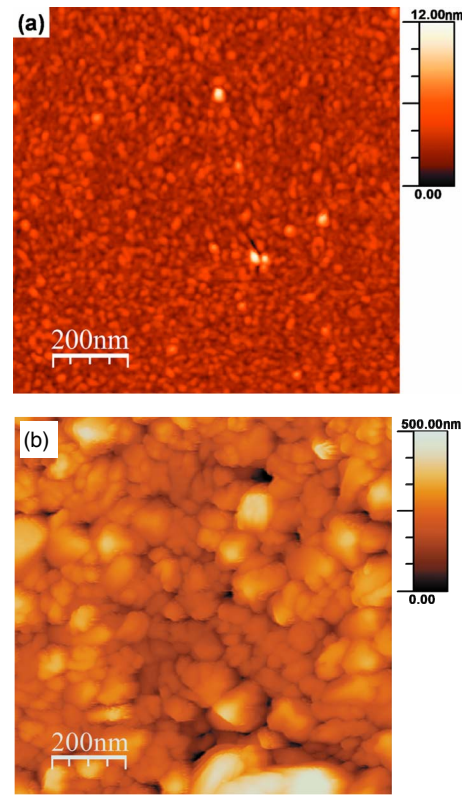


FIG. 2. (Color online) AFM images of  $1 \times 1 \mu\text{m}^2$  surfaces for (a) 4 ML CuPc (rms roughness: 0.7 nm, average grain size: 21.1 nm), and (b) 1000 ML CuPc (rms roughness: 62.1 nm, average grain size: 52.7 nm).

## D. Aging and recovery experiment

The OTFTs were characterized at room temperature in an optically isolated probe station to minimize photocurrent using a voltage sweep rate of 2 V/s. The dc electrical properties were determined from current-voltage ( $I$ - $V$ ) measurements. A total of four environments were utilized to investigate the aging and recovery processes: environment I—30% relative humidity with  $\text{N}_2$ ; environment II—pure  $\text{N}_2$ ; environment III—clean dry air (20%  $\text{O}_2$ , 80%  $\text{N}_2$ ); environment I'—30% relative humidity with clean air. Water vapor was introduced into the enclosed probe station using a custom built flow system and dry  $\text{N}_2$  or clean dry air were used as carrier gases. Bubblers filled with distilled water were immersed in a 15  $^{\circ}\text{C}$  constant temperature bath and mass flow controllers were used to maintain a constant flow rate of 500 SCCM (SCCM denotes standard cubic centimeters per minute at STP) for each environment. Vapor pressure data were used with the Clausius-Clapeyron equation to calculate the concentration of water vapor in parts per million (ppm). A dose of 8440 ppm water vapor in  $\text{N}_2$  or clean dry air carrier gas was used to create a relative humidity of roughly 30%.

## III. RESULTS AND DISCUSSION

Bottom contact OTFTs were prepared with channel thicknesses of 4 ML and 1000 ( $\pm 5\%$ ) ML CuPc films to investigate the effects of aging on films with different surface microstructure. Schematic cross sections of the bottom contact OTFTs fabricated by the bilayer photoresist lift-off

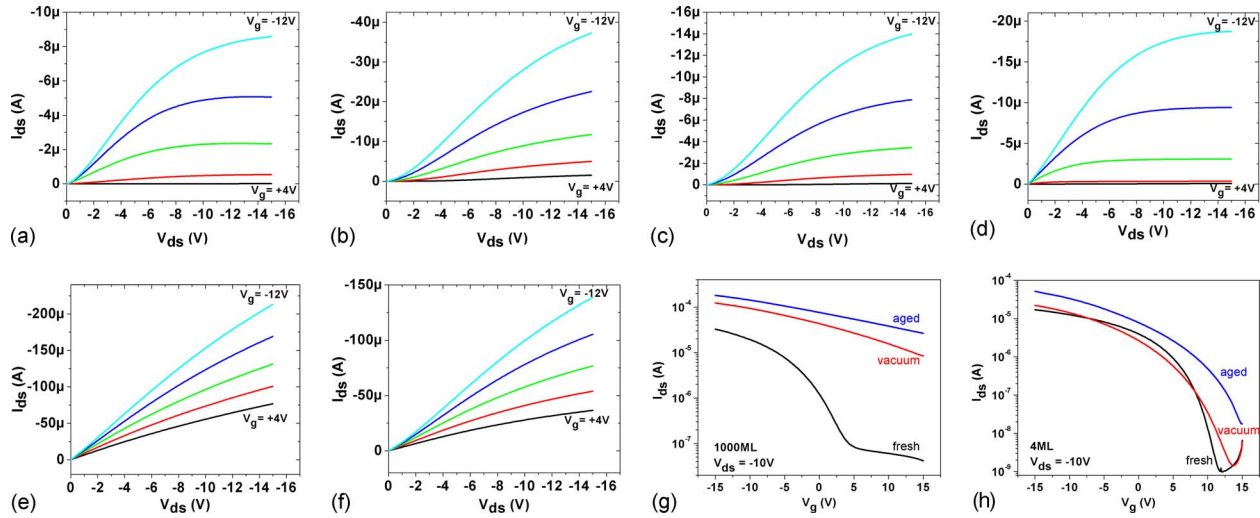


FIG. 3. (Color online) Output characteristics of 4 ML CuPc [(a)–(c)] vs 1000 ML CuPc [(d)–(f)] OTFTs. [(a) and (d)] as-prepared fresh devices, [(b) and (e)] after aging in the ambient air for 14 days (average relative humidity  $\sim 50\%$ ), [(c) and (f)] after 4 days in a high vacuum ( $10^{-7}$  Torr) chamber. Transfer data for 4 ML CuPc (h) and 1000 ML CuPc (g).

process<sup>19</sup> are shown in Fig. 1. AFM images of (a) 4 ML CuPc and (b) 1000 ML CuPc films are shown in Fig. 2. The root-mean-square (rms) roughnesses are 0.7 and 64.4 nm for 4 ML CuPc and 1000 ML CuPc films. The rms roughness increases linearly with film thickness with a slope of 0.06 nm/ML. For the 1000 ML films, the rms roughness is only 5% of the film thickness, which is consistent with a film of small densely packed crystallites separated by tall grain boundaries. The thick CuPc films have tall, high surface area grain boundaries which allow for more adsorption sites of oxidants ( $O_2$ ,  $NO_x$ , and  $O_3$ ) from the ambient air than a thinner CuPc layer.

OTFTs based on CuPc exhibit  $p$ -channel field-effect transistor behavior with distinct linear and saturation regions of operation, as shown by the  $I$ - $V$  characteristics in Fig. 3(d). The lower drain-source current of the 4 ML CuPc devices may be due to incomplete film coverage above the third layer or differences in film texture.<sup>16,19</sup> After 14 days in ambient air, the drain-source currents significantly increased for both 4 ML [Fig. 3(b)] and 1000 ML [Fig. 3(e)] CuPc OTFTs. The aging effects are evident in two obvious  $I$ - $V$  characteristics: increased drain-source current at  $V_g=0.0$  V and degraded saturation behavior. The aging is more dramatic in the 1000 ML CuPc OTFTs as seen in the output characteristics after 14 days in the ambient air [Fig. 3(e)]. The correlation between the film thickness and the effects of aging is consistent with fixed charge and trap state formation resulting from oxidants that are present in ambient air adsorbing in the grain boundaries.<sup>21,22</sup> To remove the traps and fixed charge, the devices were stored in a high vacuum ( $10^{-7}$  torr) chamber for 4 days. After 4 days in a high vacuum chamber, the 4 ML CuPc OTFT had improved  $I$ - $V$  characteristics relative to the aged device as shown in Fig. 3(c), while the 1000 ML CuPc OTFT retained poor  $I$ - $V$  saturation behavior with a high threshold voltage as shown in Fig. 3(f). The inability of high vacuum to induce desorption of the adsorbates causing aging is consistent with high fixed charge and trap densities forming within the deep grain boundaries of the thicker

films.<sup>9,10,23</sup> Aging the devices appears to influence injection from the contacts based on the drain-source current behavior at low drain-source voltage. In the thin CuPc devices, the nonlinear current-voltage characteristics at low drain-source voltages are attributed to a non-negligible Schottky barrier at the Au/CuPc interface. Such Schottky behavior is consistent with two possible mechanisms: (1) water adsorption lowers the HOMO level of the CuPc near the contacts, thereby creating a larger barrier to hole injection or (2) water adsorption near the contacts reduces mobile hole density due to trapping. In the thick CuPc devices the contact regions are covered with a thick CuPc layer, therefore the effects of water are minimized. The apparent Ohmic contact behavior in aged thick CuPc films is attributed to a simultaneous increase in doping concentration and fixed charge due to ambient oxidants. Previous studies have attributed a similar Ohmic conduction feature to mobile dopants.<sup>24</sup>  $NO_x$  species have large electron affinities ( $\sim 2.5$  eV) and are capable of oxidizing the CuPc to create a uniform conduction layer in the channel, even in absence of an applied gate voltage.

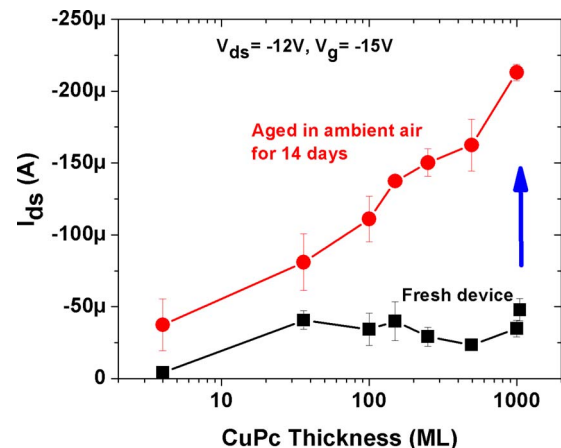


FIG. 4. (Color online) On-state current ( $I_{ds}$  at  $V_{ds} = -12$  V,  $V_g = -15$  V) with different CuPc thickness before aging (fresh) and after aging in ambient air for 14 days. Some error bars are less than the size of the data points.

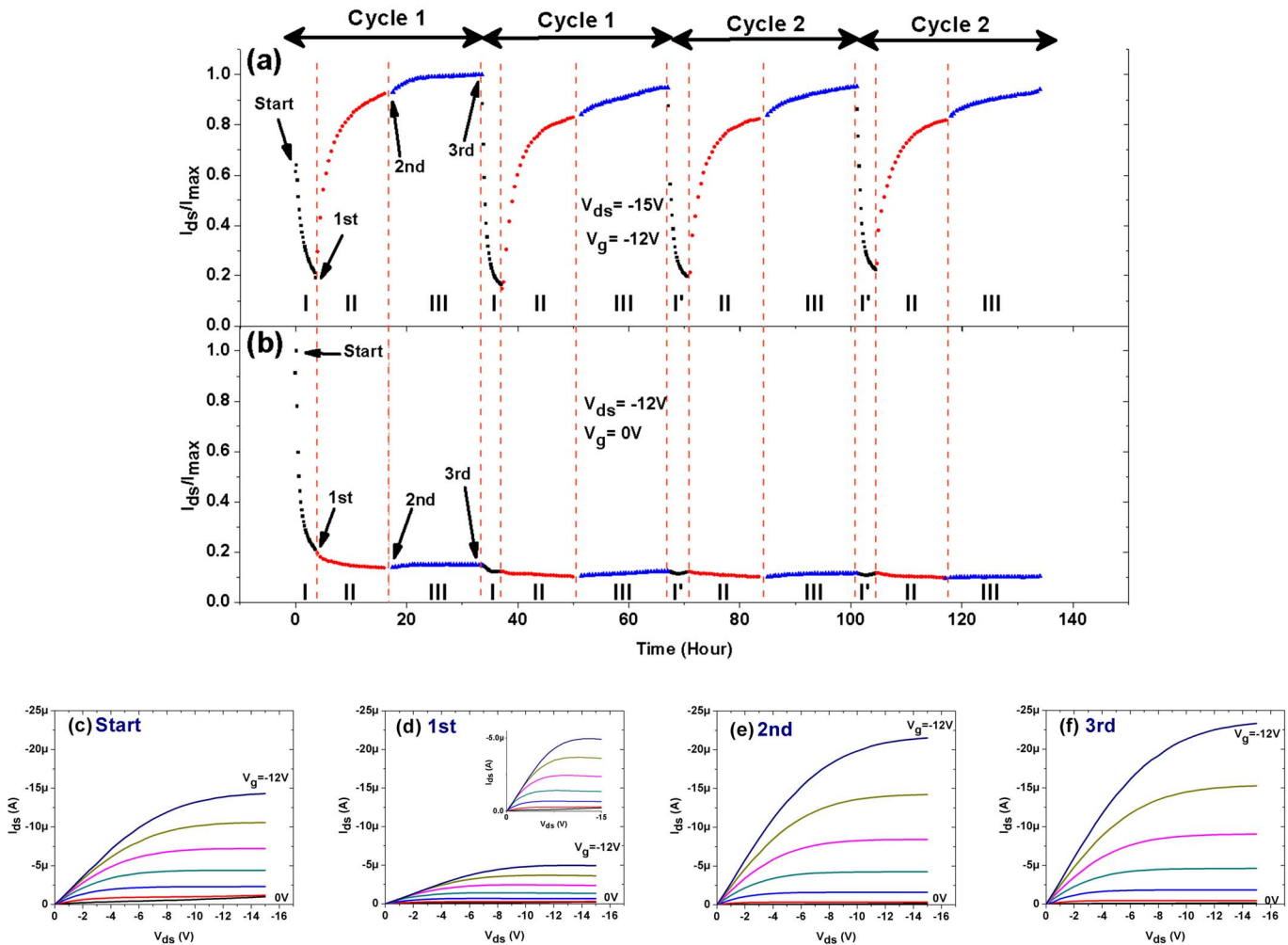


FIG. 5. (Color online) (a) On-state current (normalized to  $I_{max} = -2.33 \times 10^{-5}$  A) and (b) off-state current (normalized to  $I_{max} = -1.1 \times 10^{-6}$  A) for 1000 ML CuPc OTFTs under environment cycle 1 [environment I— $N_2$  with 30% relative humidity (3.5 h); environment II—pure  $N_2$  (13 h); environment III—clean dry air (17 h)] and environment cycle 2 [environment I'—clean air with 30% relative humidity (3.5 h); environment II—pure  $N_2$  (13 h); environment III—clean dry air (17 h)]. The output characteristics are shown at four points along cycle 1: (c) at the starting point where devices have been in the ambient air for 45 min after deposition, labeled “start,” (d) after exposure under environment I, labeled “first” (the inset shows the data on a smaller  $I_{ds}$  scale) (e) after exposure under environment II, labeled “second,” and (f) after exposure under environment III, labeled “third.” The gate voltage steps are in increments of  $-2$  V and the experiment was performed at room temperature.

The transfer data presented for 4 ML devices [Fig. 3(h)] and 1000 ML devices [Fig. 3(g)] can provide semiquantitative information relating the threshold voltage shift and trap densities in the film. For 4 ML devices, the subthreshold slope increases from  $1.5 \pm 0.5$  to  $1.9 \pm 0.1$  V/decade for fresh and aged devices, respectively, whereas for 1000 ML devices, the subthreshold slope increases from  $3.5 \pm 0.7$  to  $30.6 \pm 0.3$  V/decade for fresh and aged devices, respectively. The increased subthreshold slope is consistent with prior experimental<sup>25</sup> and theoretical<sup>26</sup> studies of impurity induced changes to electronic structure in organic thin films. Trap densities ( $N_{trap}$ ) were calculated for the fresh and aged films using  $N_{trap} = C_{ox}|V_{th} - V_{to}|/q$  (Refs. 14 and 27) where  $C_{ox}$  is the capacitance across the  $SiO_2$  gate oxide,  $V_{th}$  is the calculated threshold voltage,  $V_{to}$  is the turn-on voltage, and  $q$  is the fundamental charge. The calculated trap density for the 4 ML devices increased by  $(5.4 \pm 4.1) \times 10^{11}/cm^2$  as a result of aging; however, for 1000 ML devices the trap density increased by  $(2.4 \pm 0.3) \times 10^{12}/cm^2$ . It is noted that this calculation assumes traps are localized near the oxide/CuPc inter-

face; therefore, the calculated increase likely underestimates the true trap density since oxidants in thick films can be trapped within the bulk CuPc film. Turn-on voltages for aged 1000 ML devices were obtained by extending the gate voltage bias to  $+50$  V; however, a range of  $-15$  to  $+15$  V gate sweep is presented in Fig. 3(g) for consistency. It is noted that the minimum drain-source currents in aged 1000 ML devices is on the order of several microamperes, suggesting that the devices do not turn off due to ambient oxidants inducing fixed charge.

The on-state currents ( $V_{ds} = -12$  V,  $V_g = -15$  V) of OTFTs with different CuPc channel thickness before aging and after aging in ambient air for 14 days are given in Fig. 4. Before aging in ambient air, the current-voltage characteristics are independent of CuPc thickness (30 to 1000 ML), which is consistent with a charge transport mechanism in which all the carriers conduct in the first few MLs near the gate dielectric.<sup>16,28</sup> However, the on-state current of the aged OTFTs monotonically increases with CuPc thickness, consis-

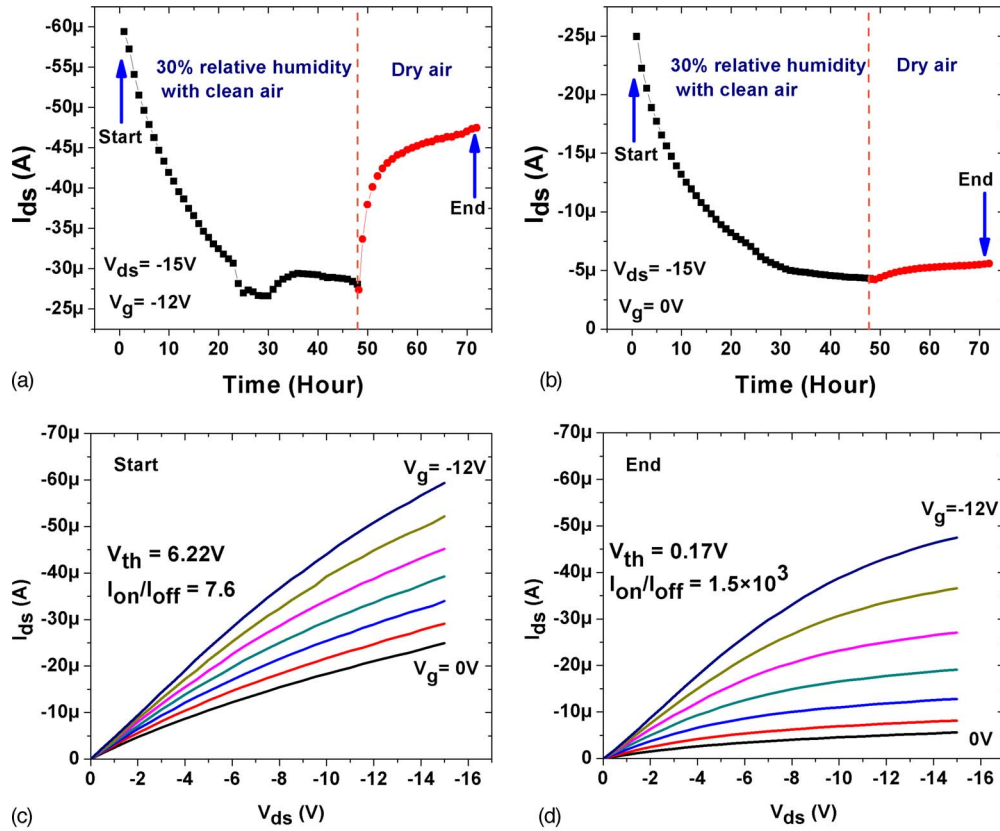


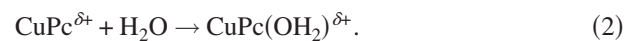
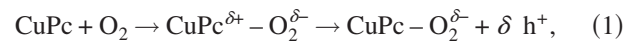
FIG. 6. (Color online) (a) On-state current at  $V_{ds} = -15$  V,  $V_g = -12$  V during the recovery test under 30% relative humidity with clean air for 48 h and clean dry air for 24 h, and (b) Off-state current at  $V_{ds} = -15$  V,  $V_g = 0$  V during the recovery test under 30% relative humidity with clean air for 48 h and clean dry air for 24 h. (c) Output characteristics of aged 1000 ML CuPc OTFTs under ambient air (d) output characteristics of aged 1000 ML CuPc OTFTs after exposure under 30% relative humidity with clean air for 48 h and clean dry air for 24 h. The gate voltage steps are in increments of  $-2$  V and the experiment was performed at room temperature.

tent with ambient oxidants adsorbing in grain boundaries and forming negative fixed charge and a high trap density in the film.<sup>29,30</sup>

Thick CuPc devices exhibited the most dramatic effects of aging and were used for isolating the cause of aging in ambient air. Exposure of 1000 ML thick CuPc OTFTs to two environment cycles isolated the causes of device degradation. Figure 5(a) shows the on-state current (normalized to  $I_{max} = -2.33 \times 10^{-5}$  A) and Fig. 5(b) shows the off-state current (normalized to  $I_{max} = -1.1 \times 10^{-6}$  A) for the two different environment cycles. Cycle 1 employs three environments over 33.5 h: environment I—30% relative humidity with  $N_2$  (3.5 h); environment II—pure  $N_2$  (13 h); and environment III—clean dry air (17 h). Cycle 2 employs the same three environments with the exception that environment I is replaced with environment I'—30% relative humidity with clean air. The cycles were repeated to confirm reproducibility. Three devices were individually tested using identical exposure cycles. The on-state current at the end of the experiments had a deviation of less than 30%. The variability in on-state current is attributed to variability in the strong oxidants present in ambient conditions which influence the initial output characteristics. The off-state current is consistently reduced to negligibly small values following the initial exposure to clean humidified environments.

The effects of each environment can be summarized by the following: Environments I and I' initiate each cycle by

decreasing the output current via the adsorption of water. Next, exposure to pure  $N_2$  in environment II facilitates the desorption of water so the output current increases. Finally, exposure to dry air in environment III causes a further increase in output current due to doping by  $O_2$ . The results in Fig. 5(a) are consistent with an  $O_2$  and  $H_2O$  doping mechanism for  $p$ -type CuPc films.  $O_2$  in clean dry air increases the CuPc film conductivity by acting as the primary dopant<sup>29,31</sup> [Eq. (1)] and  $H_2O$  decreases conductivity acting as a counter-dopant [Eq. (2)].<sup>31,32</sup> In Eq. (2), water forms a complex with  $CuPc^{\delta+}$  to stabilize the mobile holes and decrease conductivity in the film.<sup>33</sup>



The partial charge separation in Eq. (1) represents partial electron transfer between the CuPc and  $O_2$ , consistent with density functional theory (DFT) calculations for charge transfer between organic vapor analytes and zinc phthalocyanine.<sup>34</sup> DFT calculations for  $O_2$  binding to cobalt phthalocyanine (CoPc) show small electron transfer from CoPc to  $O_2$  (0.28 electrons) and a binding energy of 0.98 eV, suggesting that charge transfer to the CuPc is not restricted by energy level alignment between  $O_2$  and CuPc.<sup>35</sup> Although the reported electron transfer for strong oxidants such as NO

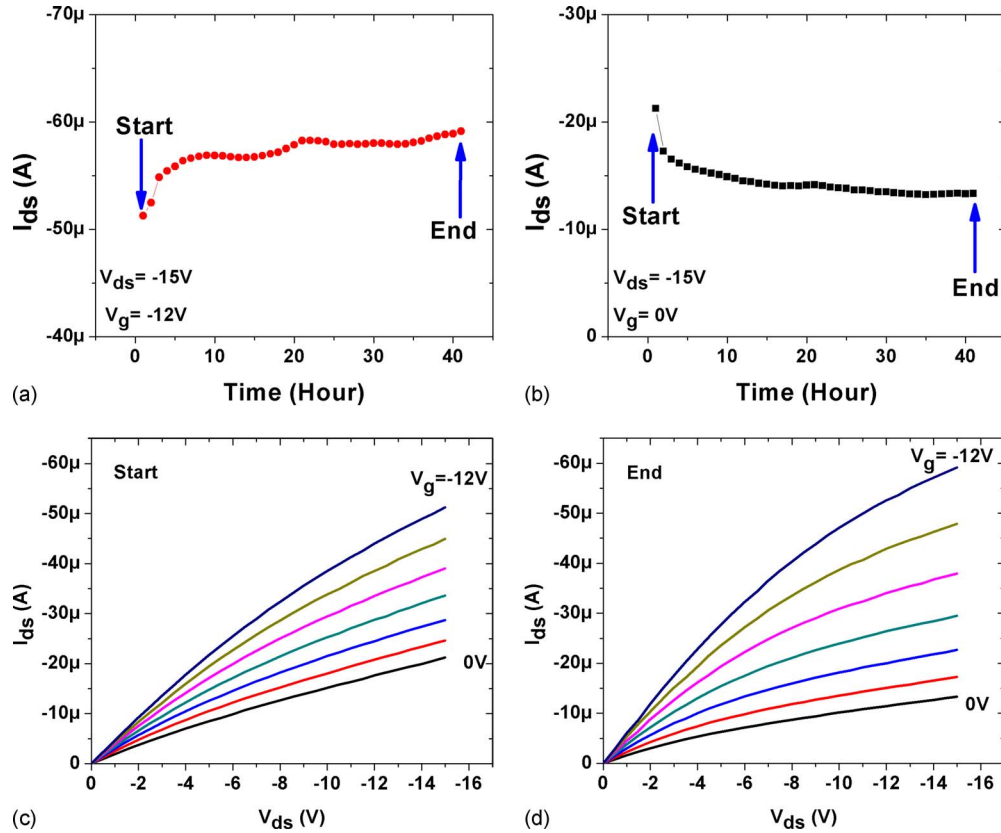


FIG. 7. (Color online) (a) Drain-source current at  $V_{ds} = -15$  V,  $V_g = -12$  V in clean dry air for 41 h, (b) drain-source current at  $V_{ds} = -15$  V,  $V_g = 0$  V in clean dry air for 41 h. (c) Output characteristics of aged 1000 ML CuPc OTFTs under ambient air and (d) output characteristics of aged 1000 ML CuPc OTFTs after exposure to clean dry air for 41 h. The drain-source current in clean dry air does not change significantly. The gate voltage steps are in increments of  $-2$  V and the experiment was performed at room temperature.

on iron phthalocyanine films are comparable to that of  $O_2$  (0.26 electrons), the binding energy is significantly larger ( $E_{bind} = 1.69$  eV). Therefore, the observed threshold voltage shift appears to be strongly correlated with tight binding oxidants which form fixed charge in the film microstructure.

To understand the role of  $O_2$  and  $H_2O$  with respect to the fixed charge and threshold voltage, the  $I$ - $V$  output characteristics at each environment transition are shown for cycle 1 in Figs. 5(c)–5(f). Note that the sequences in Figs. 5(a) and 5(b) are initiated using a device that had been exposed to ambient conditions for 45 min after CuPc deposition. By comparing Figs. 5(c) and 5(f), it is apparent that the effects of aging are not caused by  $O_2$ , nor by  $H_2O$ , but are reversed by these species since Fig. 5(f) shows a lower off-state drain-source current at  $V_g = 0.0$  V than Fig. 5(c). Similar output characteristics are obtained at each of the environment cycles. The well-behaved device characteristics demonstrated throughout the 4 cycles indicate that the large threshold voltage and poor saturation behavior in aged devices are due to trace strong oxidants (e.g.,  $O_3$  and  $NO_x$ ) in ambient air and not due to any combination of  $O_2$  and  $H_2O$ . Instead, it is likely that  $H_2O$  displaces or reacts with the trace strong oxidants thereby allowing only  $O_2$  to dope the film in environment III.

Most adsorption sites are readily accessible to the gas molecules because they are located at the air/MPc interface at coherent and incoherent step edges. However, there are also less accessible adsorption sites in grain boundaries. Water causes a decrease in current due to donation of electron

pairs from water molecules to the  $p$ -type film,<sup>32</sup> and diffusion of  $H_2O$  in and out of grain boundaries is expected to be slow. Therefore, the 1000 ML OTFTs require prolonged exposure in a water-free environment for full recovery from exposure to humid environments.

Long exposure to water vapor is key to the reversal of aging since water has a moderate binding strength<sup>34</sup> and must displace strong oxidants via diffusion in grain boundaries. To demonstrate that humidified clean air can induce recovery from ambient exposure, aged 1000 ML CuPc OTFTs were exposed to 30% relative humidity with clean air for 48 h and clean dry air for 24 h. The on-state and off-state currents during the recovery sequence are plotted in Figs. 6(a) and 6(b), respectively. Figure 6(c) shows the representative output characteristics for aged 1000 ML CuPc OTFTs with the typical aging characteristics; a lack of current saturation and high drain-source current at  $V_g = 0.0$  V. The device performance of the recovered 1000 ML CuPc OTFTs is shown in Fig. 6(d) after exposure to clean humidified and clean dry air. The long time for recovery is characteristic of 1000 ML thick devices. Recovery was demonstrated on three aged devices with similar initial output characteristics; the deviation in saturation current between devices was less than 20% at both the beginning and end of the recovery sequence. After exposure to the clean controlled environments, the devices have relatively good saturation behavior even at high gate voltage and a low threshold voltage as shown in Fig. 6(d). The recovery process was able to lower the threshold

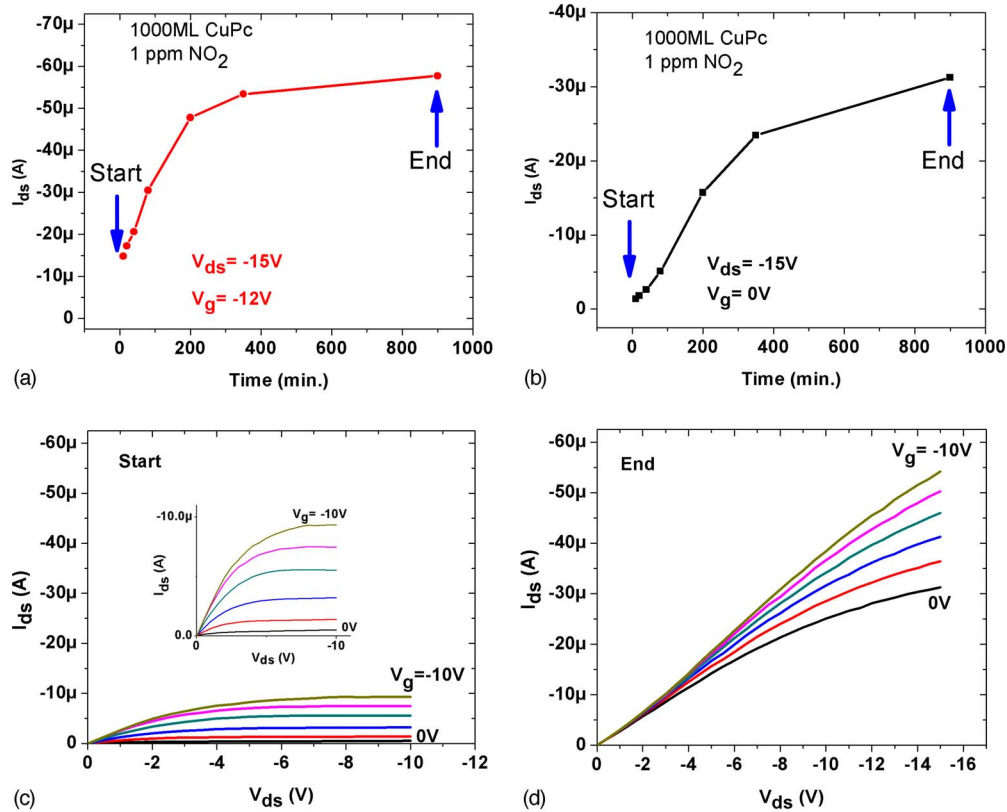


FIG. 8. (Color online) (a) On-state current for 1000 ML CuPc OTFT exposed to 1 ppm  $\text{NO}_2$ ; (b) off-state current for 1000 ML CuPc OTFT exposed to 1 ppm  $\text{NO}_2$ . (c) Output characteristics of a fresh 1000 ML OTFT exposed to ambient conditions for  $\sim 10$  min (the inset shows the data on a smaller  $I_{ds}$  scale). (d) Output characteristics of the same device after 900 min exposure to the 1 ppm  $\text{NO}_2$  environment. The gate voltage steps are in increments of  $-2$  V and the experiment was performed at room temperature.

voltage by about  $35\times$  (from 6.22 to 0.17 V), improve the on/off ratio by about  $200\times$  (from 7.6 to  $1.5\times 10^3$ ), and decrease the current slope at saturation by about  $100\times$  (from  $2\times 10^{-6}$  A/V to  $7\times 10^{-8}$  A/V at  $V_g = -6$  V). The mobility decreased by only  $1.6\times$  (from  $1.1\times 10^{-3}$  to  $0.7\times 10^{-3}$   $\text{cm}^2 \text{V}^{-1} \text{s}^{-1}$ ) following the recovery, which is consistent with fixed charge primarily influencing the on/off ratio and threshold voltage in OTFTs. These results suggest that strong oxidant adsorption can be reversed by exposure to another strong chemisorbate such as  $\text{H}_2\text{O}$ .

The responses of aged 1000 ML CuPc OTFTs to a water-free environment were investigated to confirm the role of  $\text{H}_2\text{O}$  in the recovery process. The aged devices [ $I$ - $V$  output plotted in Fig. 7(c)] were exposed to clean dry air for 41 h [Figs. 7(a) and 7(b)]. As shown in Fig. 7(d), clean dry air could not restore the devices which retained high threshold voltages and poor saturation at high gate voltages.

To confirm that trace strong oxidants in ambient air are responsible for the aging process, 1000 ML CuPc OTFTs were measured following exposure to a simulated ambient environment containing clean dry air and 10 ppm  $\text{NO}_2$  in clean dry air (Airgas) in a 10:1 mixture, leading to a net  $\text{NO}_x$  concentration of 1 ppm. It is noted that  $\text{NO}_2$  exists as both a monomer and dimer, and  $\text{NO}_2$  gas usually contains NO impurities so the gas is referred to as  $\text{NO}_x$ . Figures 8(a) and 8(b) depict the evolution over time of the on- and off-state currents. The fresh device shown in Fig. 8(c) shows characteristic linear and saturation behavior of a well behaved

OTFT. After exposure to 1 ppm  $\text{NO}_x$  for 900 min the device has poor output characteristics [see Fig. 8(d)], which are almost identical to the output characteristics for devices that have been exposed for two weeks to ambient air [see Fig. 3(e)]. The  $V_g = 0.0$  V curve in Fig. 8(b) indicates formation of fixed charge resulting in a large threshold voltage. It is noted that ambient air typically contains only 30 ppb of  $\text{NO}_x$  so exposure to 900 min at 1 ppm  $\text{NO}_x$  is similar to exposure to 50 h of ambient  $\text{NO}_x$ . These results support an aging mechanism which is dependent on the level of strong oxidants ( $\text{NO}_x$  and  $\text{O}_3$ ) in the atmosphere.

#### IV. SUMMARY

In summary, the aging and recovery processes in CuPc OTFTs were investigated by studying their  $I$ - $V$  output characteristics in ambient air and in controlled atmospheres. The primary aging effects in ambient air include a large increase in off-state current, a large positive threshold voltage and a loss of saturation behavior even at high gate voltage. In controlled atmospheres of clean air with and without  $\text{H}_2\text{O}$ , none of the typical aging effects are observed, consistent with  $\text{O}_2$  and  $\text{H}_2\text{O}$  not playing a direct role in the aging process. The aging process in ambient air is much more pronounced for thicker CuPc OTFTs than thin CuPc OTFTs. While the output current at high gate voltage is independent of channel thickness between 4 and 1000 ML, after aging the output current scales with channel film thickness; this is consistent

with aging being due to adsorption of trace oxidants (for example O<sub>3</sub> and NO<sub>x</sub>) at grain boundaries causing an increase in fixed charge and trap states. The adsorption of strong oxidants is reversible, since the aged devices can be restored to proper TFT behavior by prolonged exposure to humidified clean air. The thin devices are more easily restored than the thick devices, which is consistent with oxidation occurring deep in the grain boundaries for the thick film devices.

## ACKNOWLEDGMENTS

The authors thank Wilhelm Melitz who set up the LABVIEW programs for data acquisition, the Calit2 Nano3 Nanofabrication Cleanroom Facility, and the Integrated Nanosensors Laboratory at UCSD, as well as Professor Yuan Taur at UCSD for the valuable discussions. The AFOSR is acknowledged for funding under MURI Grant No. FA9550-08-1-0395 and NSF Grant No. CHE-0350571. J.P. and J.E.R. contributed equally to this work.

- <sup>1</sup>C. D. Dimitrakopoulos and P. R. L. Malenfant, *Adv. Mater. (Weinheim, Ger.)* **14**, 99 (2002).
- <sup>2</sup>G. Horowitz, *Adv. Mater. (Weinheim, Ger.)* **10**, 365 (1998).
- <sup>3</sup>R. D. Yang, J. Park, C. N. Colesniuc, I. K. Schuller, W. C. Trogler, and A. C. Kummel, *J. Appl. Phys.* **102**, 034515 (2007).
- <sup>4</sup>F. Liao, C. Chen, and V. Subramanian, *Sens. Actuators B* **107**, 849 (2005).
- <sup>5</sup>J. B. Chang, V. Liu, V. Subramanian, K. Sivula, C. Luscombe, A. Murphy, J. Liu, and J. M. J. Frechet, *J. Appl. Phys.* **100**, 014506 (2006).
- <sup>6</sup>R. Ben Chaabane, A. Ltaief, L. Kaabi, H. Ben Ouada, N. Jaffrezic-Renault, and J. Davenas, *Mater. Sci. Eng., C* **26**, 514 (2006).
- <sup>7</sup>G. Guillaud, J. Simon, and J. P. Germain, *Coord. Chem. Rev.* **178–180**, 1433 (1998).
- <sup>8</sup>S. H. Han, J. H. Kim, J. Jang, S. M. Cho, M. H. Oh, S. H. Lee, and D. J. Choo, *Appl. Phys. Lett.* **88**, 073519 (2006).
- <sup>9</sup>S. Cipolloni, L. Mariucci, A. Valletta, D. Simeone, F. De Angelis, and G. Fortunato, *Thin Solid Films* **515**, 7546 (2007).
- <sup>10</sup>D. Knipp, T. Muck, A. Benor, and V. Wagner, *J. Non-Cryst. Solids* **352**, 1774 (2006).
- <sup>11</sup>Y. Qiu, Y. Hu, G. Dong, L. Wang, J. Xie, and Y. Ma, *Appl. Phys. Lett.* **83**, 1644 (2003).
- <sup>12</sup>Z.-T. Zhu, J. T. Mason, R. Dieckmann, and G. G. Malliaras, *Appl. Phys. Lett.* **81**, 4643 (2002).
- <sup>13</sup>C. R. Kagan, A. Afzali, and T. O. Graham, *Appl. Phys. Lett.* **86**, 193505 (2005).
- <sup>14</sup>Y. Natsume, *Phys. Status Solidi A* **205**, 2958 (2008).
- <sup>15</sup>T. Someya, H. E. Katz, A. Gelperin, A. Lovinger, and A. Dodabalapur, *Appl. Phys. Lett.* **81**, 3079 (2002).
- <sup>16</sup>R. D. Yang, T. Gredig, C. N. Colesniuc, J. Park, I. K. Schuller, W. C. Trogler, and A. C. Kummel, *Appl. Phys. Lett.* **90**, 263506 (2007).
- <sup>17</sup>C. Clarisse and M. T. Riou, *J. Appl. Phys.* **69**, 3324 (1991).
- <sup>18</sup>X. Yan, H. Wang, and D. Yan, *Thin Solid Films* **515**, 2655 (2006).
- <sup>19</sup>J. Park, R. D. Yang, C. N. Colesniuc, A. Sharoni, S. Jin, I. K. Schuller, W. C. Trogler, and A. C. Kummel, *Appl. Phys. Lett.* **92**, 193311 (2008).
- <sup>20</sup>C. W. Miller, A. Sharoni, G. Liu, C. N. Colesniuc, B. Frubberger, and I. K. Schuller, *Phys. Rev. B* **72**, 104113 (2005).
- <sup>21</sup>J. Steiger, S. Karg, R. Schmechel, and H. von Seggern, *Synth. Met.* **122**, 49 (2001).
- <sup>22</sup>L. Torsi, M. C. Tanese, N. Cioffi, M. C. Gallazzi, L. Sabbatini, P. G. Zamboni, G. Raos, S. V. Meille, and M. M. Giangregorio, *J. Phys. Chem. B* **107**, 7589 (2003).
- <sup>23</sup>J. B. Chang and V. Subramanian, *Appl. Phys. Lett.* **88**, 233513 (2006).
- <sup>24</sup>G. Horowitz, *Adv. Mater. (Weinheim, Ger.)* **8**, 177 (1996).
- <sup>25</sup>R. A. Street, M. L. Chabinyc, and F. Endicott, *Phys. Rev. B* **76**, 045208 (2007).
- <sup>26</sup>N. L. Tran and A. C. Kummel, *J. Chem. Phys.* **127**, 214701 (2007).
- <sup>27</sup>K. P. Pernstich, S. Haas, D. Oberhoff, C. Goldmann, D. J. Gundlach, B. Batlogg, A. N. Rashid, and G. Schitter, *J. Appl. Phys.* **96**, 6431 (2004).
- <sup>28</sup>R. Ruiz, A. Papadimitratos, A. C. Mayer, and G. G. Malliaras, *Adv. Mater. (Weinheim, Ger.)* **17**, 1795 (2005).
- <sup>29</sup>R. Rella, A. Serra, P. Siciliano, A. Tepore, L. Valli, and A. Zocco, *Langmuir* **13**, 6562 (1997).
- <sup>30</sup>J. D. Wright, *Prog. Surf. Sci.* **31**, 1 (1989).
- <sup>31</sup>R. D. Yang, J. Park, C. Colesniuc, I. K. Schuller, J. E. Royer, W. C. Trogler, and A. C. Kummel, *J. Chem. Phys.* **130**, 164703 (2009).
- <sup>32</sup>A. Belghachi and R. A. Collins, *J. Phys. D* **21**, 1647 (1988).
- <sup>33</sup>F. I. Bohrer, A. Sharoni, C. Colesniuc, J. Park, I. K. Schuller, A. C. Kummel, and W. C. Trogler, *J. Am. Chem. Soc.* **129**, 5640 (2007).
- <sup>34</sup>N. L. Tran, F. I. Bohrer, W. C. Trogler, and A. C. Kummel, *J. Chem. Phys.* **130**, 204307 (2009).
- <sup>35</sup>M. Honda, K. Kanai, K. Komatsu, Y. Ouchi, H. Ishii, and K. Seki, *J. Appl. Phys.* **102**, 103704 (2007).